COMPEL - The international journal for computation and mathematics in electrical and electronic engineering

SEMICONDUCTOR DEVICE MODELLING FOR HETEROJUNCTIONS STRUCTURES WITH MIXED FINITE ELEMENTS

F. Hecht, A. Marrocco, E. Caquot, M. Filoche,

COMPEL - The International Journal for Computation and Mathematics in Electrical and Electronic Engineering
Vol 10, No 4, 425-438 (c) James & James Science Publishers Ltd

SEMICONDUCTOR DEVICE MODELLING FOR HETEROJUNCTIONS STRUCTURES WITH MIXED FINITE ELEMENTS

F. Hecht, A. Marrocco
INRIA Domaine de Voluceau - Rocquencourt
BP 105 78153 LE CHESNAY FRANCE

and

E. Caquot, M. Filoche
CNET 196 avenue H.Ravera
92220 BAGNEUX FRANCE

Abstract

Numerical simulation of the static semiconductor device equations using mixed finite element for the approximation and A.D.I. techniques (Douglas-Rachford with local time steps) for the solution is presented in this paper. The formulation with electrostatic potential φ and quasi-Fermi levels φ_n, φ_p is used.

1 Introduction

Numerical results related to the simulation of electrical behaviour of heterojunction semiconductor devices via mixed finite element are presented. We start from the classical static equations governing this behaviour, written with the **electrostatic potential** φ and the **quasi-Fermi levels** φ_n, φ_p (for electrons and holes respectively), i.e. the following nonlinear partial differential system of equations [1][2]

$$-div(\varepsilon grad\varphi) + q\Big(\mathrm{N}(\varphi,\varphi_n) - \mathrm{P}(\varphi,\varphi_p) - dop\Big) = 0 \tag{1.1}$$

$$-div\Big(q\mu_n \mathrm{N}(\varphi,\varphi_n) grad\varphi_n\Big) + q\mathrm{U}(\varphi,\varphi_n,\varphi_p) = 0 \tag{1.2}$$

$$-div\Big(q\mu_p \mathrm{P}(\varphi,\varphi_p) grad\varphi_p\Big) - q\mathrm{U}(\varphi,\varphi_n,\varphi_p) = 0 \tag{1.3}$$

These equations are completed with boundary conditions which are in general, non-homogeneous Dirichlet conditions for φ, φ_n and φ_p on some parts of the boundary (ohmics contacts) and homogeneous Neumann conditions on the other parts. The system (1.1)-(1.3) is then written in an equivalent way by introducing the **flux variables** as dependent variables so a new system with 6 unknowns $(\varphi, \vec{\mathrm{D}}, \varphi_n, \mathbf{J}_n, \varphi_p, \mathbf{J}_p)$ is obtained. A weak formulation of the last system is used for a finite element approximation (Raviart-Thomas mixed finite elements [4]) It is well known that as particular case, (when no external potential is applied i.e. - equilibrium state-), the non linear Poisson equation (1.1) only

has to be considered; in this case φ_n and φ_p appear as constant parameters (typically $\varphi_n \equiv \varphi_p \equiv 0$). A detailed implementation of such finite elements is given in that particular case; the resulting saddle point problem is solved by the use of an A.D.I. technique (Douglas-Rachford algorithm which may be considered as a variant of UZAWA algorithm within the context of augmented lagrangian [5][6][7][8], in which the use of a *local time step (or homogenized penalization)* leads to an *efficient iterative procedure* for the solution of such nonlinear problems.

In (1.1)-(1.3), $\mathrm{N}(\varphi,\varphi_n)$, $\mathrm{P}(\varphi,\varphi_p)$ are respectively the electron and hole concentrations; typical models for these non-linear functions can be found in [1][2][3], as well as for the mobilities μ_n and μ_p and the generation/recombination term $\mathrm{U}(\varphi,\varphi_n,\varphi_p)$. Extension of the numerical procedure to the set of equations (1.1)-(1.3) is considered and numerical results presented.

2 Numerical solution of non linear Poisson equation using mixed finite elements.

2.1 Problem formulation and solution

As in [9] let us describe the framework of mixed finite element approximation and solution by an A.D.I. technique of the non linear Poisson equation. We start from the problem: Find φ solution of

$$-div(\varepsilon grad\varphi) + F(\varphi) = 0 \tag{2.1}$$

with the boundary conditions

$$\frac{\partial\varphi}{\partial n} = g_n \quad on \quad \Gamma_n \subset \partial\Omega \tag{2.2}$$

$$\varphi = g_d \quad on \quad \Gamma_d \subset \partial\Omega \tag{2.3}$$

Note that $\Gamma_d = \partial\Omega - \Gamma_n$ and that

$$F(\varphi) = F_{\varphi_n,\varphi_p}(\varphi) = q\Big(\mathrm{N}(\varphi,\varphi_n) - \mathrm{P}(\varphi,\varphi_p) - dop\Big) \tag{2.4}$$

with $\varphi_n \equiv \varphi_p \equiv 0$.

F(.) is an increasing function (see for example fig 1 for GaAs material).

The problem (2.1)-(2.3) is written in an equivalent way by intoducing the flux variable $\bar{\mathrm{D}}$ as dependent variable: Find $\bar{\mathrm{D}}$ and φ such that

$$-div(\bar{\mathrm{D}}) + F(\varphi) = 0 \quad in \quad \Omega \tag{2.5}$$

$$\bar{\mathrm{D}} = \varepsilon grad\varphi \quad in \quad \Omega \tag{2.6}$$

$$\bar{\mathrm{D}}.\mathrm{n} = \varepsilon g_n \quad on \quad \Gamma_n \tag{2.7}$$

$$\varphi = g_d \quad on \quad \Gamma_d \tag{2.8}$$

Let us consider the following Sobolev spaces

$$\mathbf{H}(div) = \{\mathbf{q} \mid \mathbf{q} \in (L^2(\Omega))^2, \quad div(\mathbf{q}) \in L^2(\Omega)\} \tag{2.9}$$

$$\mathbf{V}_0 = \{\mathbf{q} \mid \mathbf{q} \in \mathbf{H}(div), \quad \mathbf{q}.\mathbf{n} = 0 \quad on \quad \Gamma_n\} \tag{2.10}$$

For sufficiently regular given data, we obtain an equivalent weak formulation of the problem (2.5)-(2.8)
Find $\bar{\mathbf{D}} \in \mathbf{H}(div)$ and $\varphi \in L^2(\Omega)$ such that

$$-\int_\Omega v.div\bar{\mathbf{D}}dx + \int_\Omega v.F(\varphi)dx = 0 \quad \forall v \in L^2(\Omega) \tag{2.11}$$

$$\int_\Omega \mathbf{q}.[\varepsilon]^{-1}\bar{\mathbf{D}}dx = -\int_\Omega \varphi.div\mathbf{q}dx + \int_{\Gamma_d} g_d\mathbf{q}.\mathbf{n}d\Gamma \quad \forall \mathbf{q} \in \mathbf{V}_0 \tag{2.12}$$

with the condition

$$\bar{\mathbf{D}}.\mathbf{n} = \varepsilon g_n \quad on \quad \Gamma_n$$

In general for the applications we have $g_n = 0$, so we seek for $\bar{\mathbf{D}} \in \mathbf{V}_0$.
The weak formulation (2.11)-(2.12) is used for finite element approximation; following [4] we define finite dimensional subspaces of $L^2(\Omega)$ and $\mathbf{H}(div)$ constructed over a triangulation $\mathcal{T}_h$ of Ω (for example in 2D).

$$L_h = \{v_h \in L^2(\Omega) \mid \forall K \in \mathcal{T}_h, \quad v_h|_K = c^{te}\} \tag{2.13}$$

$$\mathbf{V}_h = \{\mathbf{q}_h \in \mathbf{H}(div) \mid \forall K \in \mathcal{T}_h, \quad \mathbf{q}_h(x,y)|_K = \begin{vmatrix}\alpha_K \\ \beta_K\end{vmatrix} + \gamma_K \begin{vmatrix} x \\ y \end{vmatrix}\} \tag{2.14}$$

We suppose that Γ_n is obtained by union of boundary edges of the triangular mesh $\mathcal{T}_h$ and that

$$\mathbf{V}_{0h} = \mathbf{V}_0 \cap \mathbf{V}_h \tag{2.15}$$

i.e.

$$\mathbf{V}_{0h} = \{\mathbf{q}_h \mid \mathbf{q}_h \in \mathbf{V}_h, \quad \mathbf{q}_h.\mathbf{n} = 0 \quad on \quad \Gamma_n\} \tag{2.16}$$

The formulation of the discrete problem is obvious from (2.11)-(2.15).
The problem (2.11)-(2.12) (both in continuous and discrete case) is a saddle point problem and as in [5][6] for example, we can found that these equations are the stationary conditions of a Lagrangian. Following the same techniques as in [5][6], Augmented Lagrangian can be associated and some variants of the UZAWA algorithm (named ALG2, ALG3) can be used to solve numerically such saddle point problems. As stated in [5][6][7], there is a close relation between the algorithms called ALG2 , ALG3 and the well known A.D.I. techniques (Douglas-Rachford and Peaceman-Rachford respectively) used for solving stationary elliptic problems as limit of an associated transient problem.
Let us describe here the Douglas-Rachford A.D.I. technique and point out that we find again the main feature of the augmented lagrangian approach in the solution of a class of strongly non linear elliptic partial differential equations [5][8], that is to say, the separation (decoupling) between the non linearity and the differential character of the operator.

We suppose that φ^0 and $\bar{\mathbf{D}}^0$ are given, the Douglas-Rachford algorithm (k=0,1,2,3,.....), applied to our problem is explicitely given by

- $\hat{\varphi}^{k+1} \in L_h$ solution of

$$\int_\Omega \left(\frac{\hat{\varphi}^{k+1} - \varphi^k}{\Delta t} - div\bar{\mathbf{D}}^k + F(\hat{\varphi}^{k+1}) \right).v\, dx = 0 \quad \forall v \in L_h \tag{2.16}$$

- $(\varphi^{k+1}, \bar{\mathbf{D}}^{k+1}) \in L_h \times \mathbf{V}_h$ solution of

$$\int_\Omega \left(\frac{\varphi^{k+1} - \varphi^k}{\Delta t} - div\bar{\mathbf{D}}^{k+1} + F(\hat{\varphi}^{k+1}) \right).v\, dx = 0 \quad \forall v \in L_h \tag{2.17}$$

$$\int_\Omega \mathbf{q}.[\varepsilon]^{-1}\bar{\mathbf{D}}^{k+1} dx + \int_\Omega \varphi^{k+1}.div\mathbf{q} dx = \int_{\Gamma_d} g_d \mathbf{q}.\mathbf{n} d\Gamma \quad \forall \mathbf{q} \in \mathbf{V}_{0h} \tag{2.18}$$

with the condition

$$\bar{\mathbf{D}}^{k+1}.\mathbf{n} = \varepsilon g_n \quad on \quad \Gamma_n$$

The second step in the Douglas-Rachford algorithm (given by equations (2.17) and (2.18)) leads to two decoupled problems in $\bar{\mathbf{D}}^{k+1}$ and φ^{k+1} respectively and finally a step in the Douglas-Rachford algorithm may be summarized by (Peaceman-Rachford technique and θ-scheme [6] lead to same decomposition procedures):

- a set of nonlinear (independent) equations with the unknown $\hat{\varphi}_T^{k+1}$ (one equation for each triangle of the mesh $\mathcal{T}_h$)

$$\hat{\varphi}_T^{k+1} + \Delta t.F(\hat{\varphi}_T^{k+1}) = \varphi_T^k + \Delta t.div\bar{\mathbf{D}}^k \tag{2.19}$$

- a linear problem which gives $\bar{\mathbf{D}}^{k+1}$

$$\int_\Omega \left(\mathbf{q}.[\varepsilon]^{-1}\bar{\mathbf{D}}^{k+1} + \Delta t\, div\bar{\mathbf{D}}^{k+1}.div\mathbf{q} \right) dx =$$

$$\int_\Omega \Delta t\, div\bar{\mathbf{D}}^k.div\mathbf{q}\, dx - \int_\Omega \hat{\varphi}^{k+1}.div\mathbf{q} dx + \int_{\Gamma_d} g_d \mathbf{q}.\mathbf{n} d\Gamma \quad \forall \mathbf{q} \in \mathbf{V}_{0h} \tag{2.20}$$

- φ^{k+1} is then obtained element by element with

$$\varphi_T^{k+1} = \hat{\varphi}_T^{k+1} + \Delta t.\left(div\bar{\mathbf{D}}^{k+1} - div\bar{\mathbf{D}}^k \right) \tag{2.21}$$

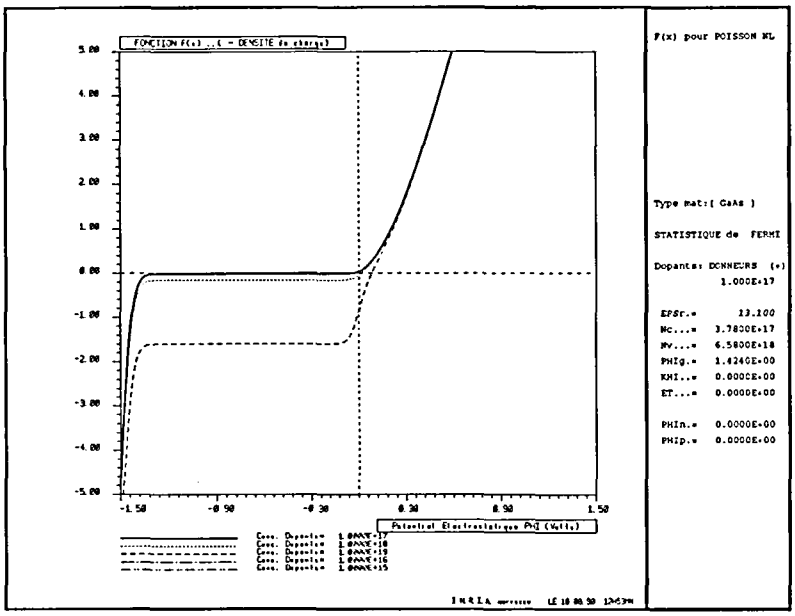

Figure 1: F function for different doping values. Material GaAs. (Fermi statistics)

2.2 Some numerical aspects

We can see on figure 1 the representation of the function F (2.4) for *GaAs* semiconductor material. The thick line represents the function for a doping value of $+10^{17}$ (donnors), the other lines for values $10^{18}, 10^{19}, 10^{16}$ and 10^{15}. The flat region of the curve (which is larger for *GaAs* than for *Ge* or *Si* -see figure 2 which gives for *Si* the representation of F with the same scaling-) directly induces numerical problems in the use of a Newton iterative process (for example) in the solution of an equation of type $F(\varphi) = constant$.

The major numerical difficulties are concentrated in the choice of the time step Δt and consequently in the choice of an (efficient) algorithm for the solution of the nonlinear equation (2.19). We are in a context in which, convergence of Douglas-Rachford algorithm is, in theory, obtained for any Δt, but of course, the speed of convergence will depend of the choice of Δt values.

Following [7] for the convergence behaviour of A.D.I. methods (or equivalently variants ALG2 or ALG3 of UZAWA methods [5][8]), it appears that a *local time step* (-a constant value by element seems a natural choice-) is appropriate and (in theory) a value given by

$$\Delta t_T = \frac{1}{F'(\varphi_T^*)} \tag{2.22}$$

where φ_T^* is the value on triangle T of the potential φ^*, solution of the problem (Poisson equation) would be optimal (*-at least near the solution-*). In fact (2.22) do not give an answer concerning the "good" choice for the time step Δt, but this formula (2.22) may

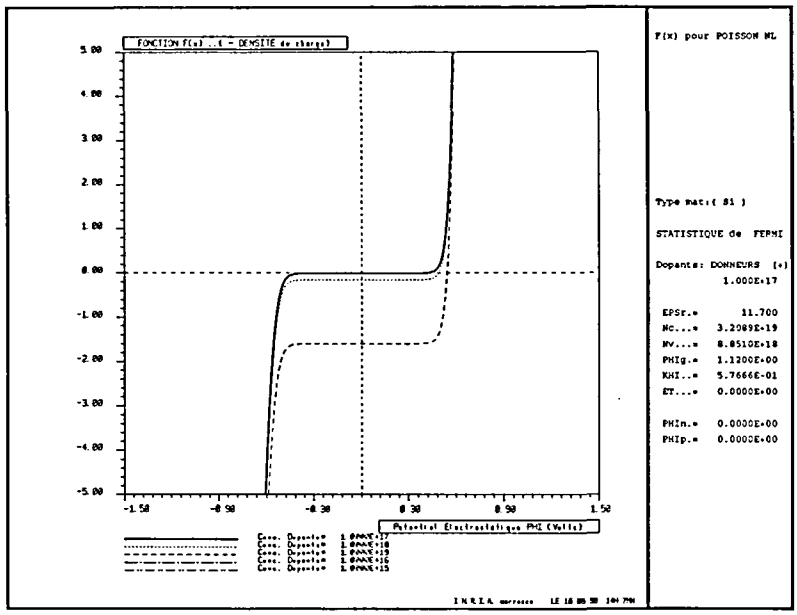

Figure 2: F function for different doping values. Material Silicium.

be used to update the time steps during the iterative process. It has to be noted that when we change the time step Δt, the matrix of the linear problem (2.20) is changed and a new factorization (costly operation in CPU time) has to be done. Other practical problems occur and are connected to the fact that on computers we work with flotting point arithmetics and some parameters cannot be choosen too large with respect to other ones. The values for the time steps given by (2.22) may be very *large* -see fig(1)- (with theoretically an infinite value when $F(\varphi)$ tends to a constant, -as for the degenerate case or limiting case,i.e. the linear Poisson equation!-). It is easy to see that if Δt is too large, in such a way that numerically the mass term $\int_\Omega q.[\varepsilon]^{-1}\bar{D}^{k+1}\,dx$ becomes negligible in comparison with the stiffness term $\int_\Omega \Delta t\, div\bar{D}^{k+1}.divq\,dx =$, then the resulting linear problem (2.20) is singular and ADI algorithm breaks down. Certainly upper bounds (derived from eq. (2.20)) have to be applied to Δt values given by (2.22); we add to relation (2.22)

$$\Delta t_T \leq \alpha \frac{S}{\varepsilon} \tag{2.23}$$

where S=area of triangle, $\alpha \sim 10^4, 10^5$ for double precision computations; this relation (2.23), derived from linear problem, seems to give satisfactory results. Stationary solutions (convergence for residuals values of type (2.24) for both φ and $\bar{D}$ of order 10^{-12}) are obtained within 50-70 Douglas-Rachford steps for any practical configurations (any usual materials and doping values). The time steps are updated periodically (each 15-20 ADI steps), so only 3-4 matrix factorizations are needed during the iterative process. We can

see on fig 3 a typical result for a $GaAs$ abrupt junction ($L_+ = 0.5\mu$, $L_- = 2.\mu$, and width $l = 0.2\mu$) ,with doping concentration values 10^{17} (for donnors) and 10^{15} (for acceptors). On figure 3 are represented:

- a) all the iterates φ^{k+1} (cut along the structure),
- b) the final solution (i.e. after ADI convergence -56steps-),
- c) the variation of residuals (of type (2.24)) for potential φ -thick line- and for $\bar{\mathrm{D}}$ -dotted line-.

$$Res\varphi = \frac{\sum_T |\varphi_T^{n+1} - \varphi_T^n|}{\sum_T |\varphi_T^{n+1}|} \tag{2.24}$$

From numerical experiments, it seems that the number of iterations in ADI algorithm needed to reach convergence is not mesh dependent.

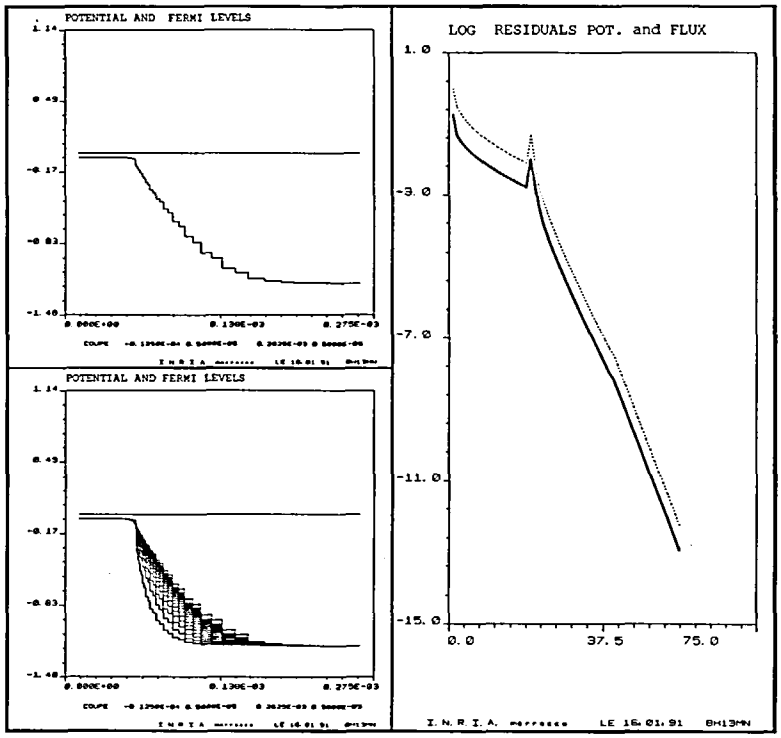

Figure 3: ADI solution for NL Poisson equation.

3 Numerical simulation including continuity equations.

The same mixed finite elements framework is used for the continuity equations. Let us recall the continuity equation for electrons (1.2) (the following can be transposed for holes equation)

$$-div\left(q\mu_n \mathrm{N}(\varphi,\varphi_n) grad\varphi_n\right) + q\mathrm{U}(\varphi,\varphi_n,\varphi_p) = 0 \quad in \quad \Omega \tag{3.1}$$

$$\frac{\partial \varphi_n}{\partial n} = gg_n \equiv 0 \quad on \quad \Gamma_n \subset \partial\Omega \tag{3.2}$$

$$\varphi_n = gg_d \quad on \quad \Gamma_d \subset \partial\Omega \tag{3.3}$$

As in the previous section, (3.1)-(3.3) is transformed on the following equivalent problem Find $\mathbf{J_n}$ and φ_n such that

$$-div(\mathbf{J_n}) + q\mathrm{U}(\varphi,\varphi_n,\varphi_p) = 0 \quad in \quad \Omega \tag{3.4}$$

$$\mathbf{J_n} = q\mu_n \mathrm{N}(\varphi,\varphi_n) grad\varphi_n \quad in \quad \Omega \tag{3.5}$$

$$\mathbf{J_n}.\mathrm{n} = 0 \quad on \quad \Gamma_n \tag{3.6}$$

$$\varphi_n = gg_d \quad on \quad \Gamma_d \tag{3.7}$$

A weak formulation is the obtained for problem (3.4)-(3.7), i.e. Find $\mathbf{J_n} \in \mathbf{H}(div)$ and $\varphi_n \in L^2(\Omega)$ such that

$$-\int_\Omega v.div\mathbf{J_n}dx + \int_\Omega v.\mathrm{U}(\varphi,\varphi_n,\varphi_p)dx = 0 \quad \forall v \in L^2(\Omega) \tag{3.8}$$

$$\int_\Omega \omega.[q\mu_n \mathrm{N}]^{-1}\mathrm{p}dx = -\int_\Omega \varphi_n.div\omega dx + \int_{\Gamma_d} gg_d\omega.\mathrm{n}d\Gamma \quad \forall \omega \in \mathbf{V_0} \tag{3.9}$$

The discrete problem is obtained by the same way as in the previous section, and the Douglas-Rachford scheme applied to this problem leads to:

- $\widehat{\varphi_n}^{k+1} \in L_h$ solution of

$$\int_\Omega \left(\frac{\widehat{\varphi_n}^{k+1} - \varphi_n^k}{\Delta t} - div\mathbf{J_n}^k + q\mathrm{U}(\varphi,\widehat{\varphi_n}^{k+1},\varphi_p)\right).v\,dx = 0 \quad \forall v \in L_h \tag{3.10}$$

- $(\varphi_n^{k+1}, \mathbf{J_n}^{k+1}) \in L_h \times \mathbf{V_{0h}}$ solution of

$$\int_\Omega \left(\frac{\varphi_n^{k+1} - \varphi_n^k}{\Delta t} - div\mathbf{J_n}^{k+1} + q\mathrm{U}(\varphi,\widehat{\varphi_n}^{k+1},\varphi_p)\right).v\,dx = 0 \quad \forall v \in L_h \tag{3.11}$$

$$\int_\Omega \omega.\left[q\mu_n \mathrm{N}(\varphi,\varphi_n^{k+1})\right]^{-1}\mathbf{J_n}^{k+1}dx + \int_\Omega \varphi_n^{k+1}.div\omega dx = \int_{\Gamma_d} gg_d\omega.\mathrm{n}d\Gamma \quad \forall \omega \in \mathbf{V_{0h}} \tag{3.12}$$

Once again, problem (3.11)-(3.12) can be decomposed. φ_n^{k+1} value is extracted from (3.11) and then using relation (3.10), we obtain

$$\varphi_n^{k+1} = \widehat{\varphi_n}^{k+1} + \Delta t.div\left(\mathrm{J_n}^{k+1} - \mathrm{J_n}^{k}\right) \tag{3.13}$$

Putting this last value in (3.12), we obtain an equation for the variable $\mathrm{J_n}^{k+1} \in \mathrm{V}_{0h}$ only:

$$\begin{aligned}\int_\Omega \omega.[q\mu_n \mathrm{N}(\varphi, \widehat{\varphi_n}^{k+1} + \Delta t.div(\mathrm{J_n}^{k+1} - \mathrm{J_n}^{k}))]^{-1}\mathrm{J_n}^{k+1}\,dx \\ + \int_\Omega \Delta t\, div\mathrm{J_n}^{k+1}.div\omega\,dx = \int_\Omega \Delta t\, div\mathrm{J_n}^{k}.div\omega\,dx \\ - \int_\Omega \widehat{\varphi}^{k+1}.div\omega dx + \int_{\Gamma_d} g_d\omega.\mathrm{n}d\Gamma \quad \forall\omega \in \mathrm{V}_{0h}\end{aligned} \tag{3.14}$$

Equation (3.14) (as well as the analogous one for holes) is non linear (the mass-matrix depends on the unknown $\mathrm{J_n}^{k+1}$) and certainly will add numerical difficulties in practical implementations.

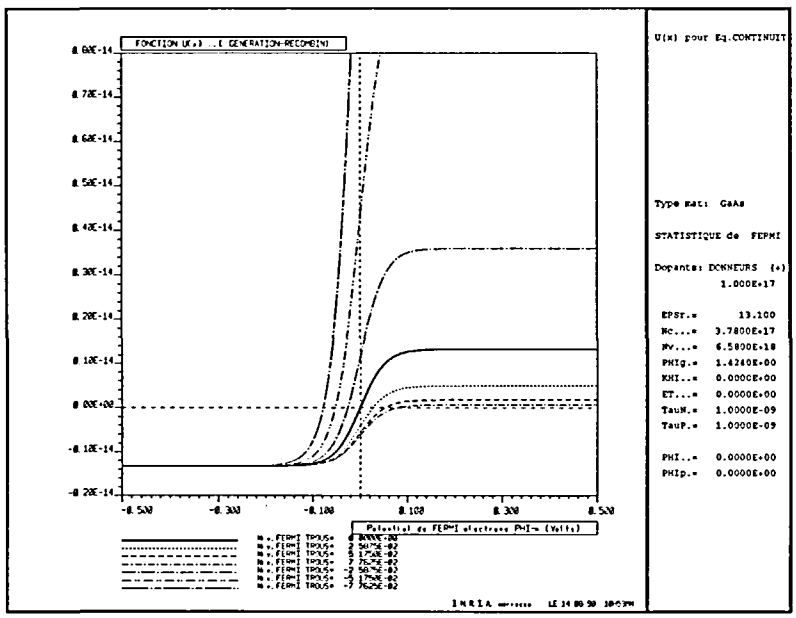

Figure 4: Representation of the S.H.R. generation/recombination.

As (2.16) or (2.19), (3.10) is a system of NT independent nonlinear equations (one equation by triangle), the function $\mathrm{F}(\varphi)$ is replaced by $U(.,\varphi_n,.)$ for which a (partial) representation (corresponding to the classical Shockley-Read-Hall generation/recombination model) is given on figure 4. The thick line represents the function U with the two others parameters ie $\varphi = 0, \varphi_p = 0$, the others curves are for different φ_p values.

Local time steps are estimated by similar techniques as for the Poisson equation, but due to the non linearity of the flux equations (like (3.14)), "good" estimations are more difficult to determine. Various numerical implementations can be considered, starting from sequential A.D.I. steps (2.19)-(2.21) , (3.10)-(3.12), .., for $\varphi, \bar{\mathrm{D}}$, φ_n, J_n, φ_p, J_p, combined with fixed point algorithm for (3.14) (and analogous one for holes), to more implicit schemes by replacing, for example, sequential independant equations (2.19) (3.10) (and analogous one for the holes), by a coupled 3x3 nonlinear equations for variables $\hat{\varphi}_T^{k+1}, \hat{\varphi}_{n_T}^{k+1}, \hat{\varphi}_{p_T}^{k+1}$, and solving non linear problems of type (3.14) by more sophisticated techniques.

Partial numerical results are presented in the following. We use (Douglas-Rachford) A.D.I. steps sequentially for Poisson, electron continuity, hole continuity equations. Newton type algorithm is used for the non linear equations with $\hat{\varphi}^{k+1}$ (or $\hat{\varphi}_n^{k+1}$, or $\hat{\varphi}_p^{k+1}$) unknown. The non linear flux equations (type (3.14)) are solved via fixed point algorithm.

We consider the *GaAs* diode described previously with non zero applied potential at ohmic contacts. No generation-recombination term is considered in this numerical application ($\mathbf{U} \equiv 0$).

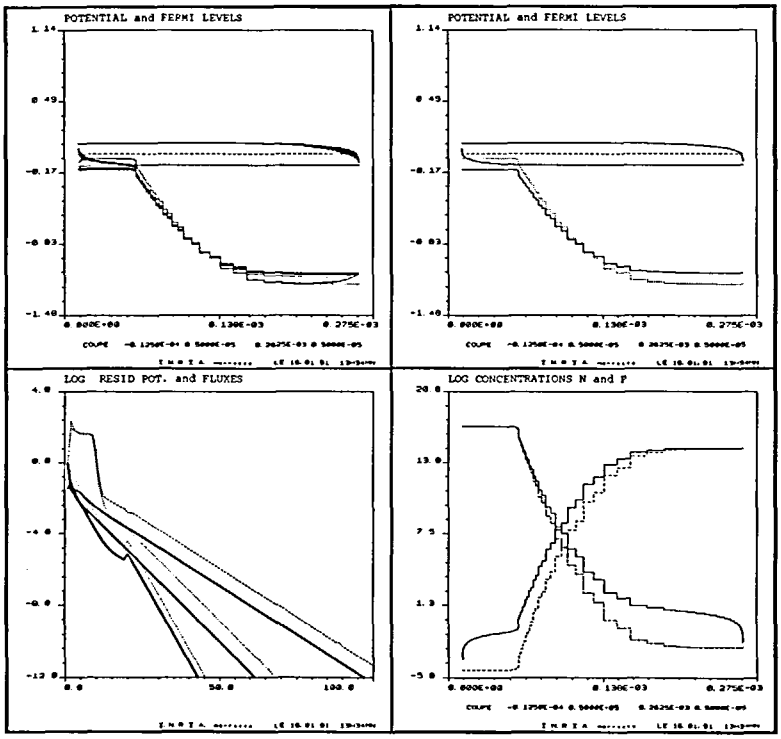

Figure 5: Forward bias (GaAs diode) 0.2V

- **Forward bias**

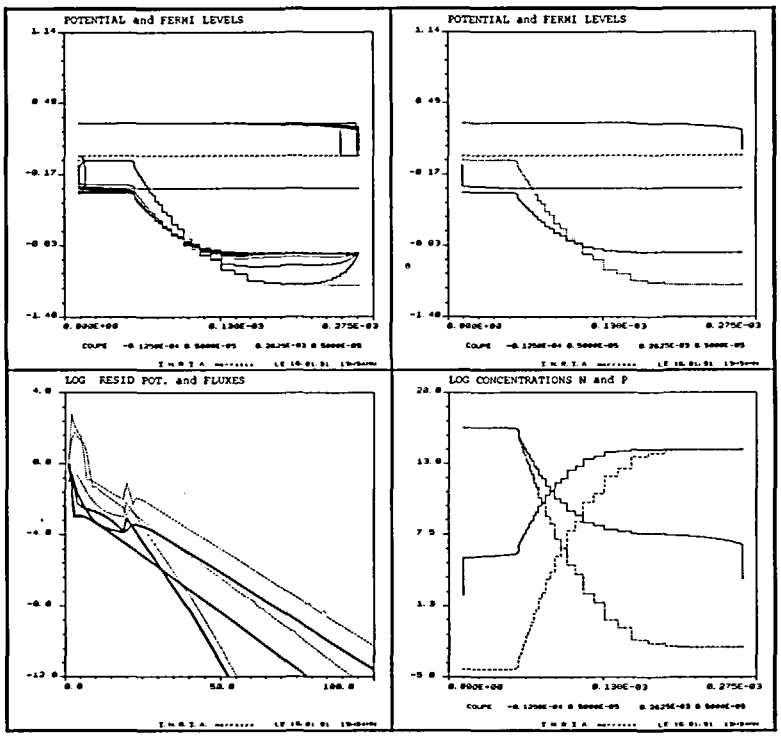

Figure 6: Forward bias (GaAs diode) 0.6V

We can see on figures (5, 6) the results obtained in the case of 0.2V and 0.6V forward bias. For both numerical simulations the initial state for the ADI algorithm is the equilibrium state (we can also proceed by continuation on applied voltage and taking as initial state, the solution at previous bias).

The following numerical results are reported on fig.(5, 6):

- a) evolution of electrostatic potential and Fermi levels during ADI steps.
- b) the final solution (together with initial solution -dotted lines-).
- c) the decrease of residuals (log. scale) for all variables $\varphi, \varphi_n, \varphi_p$ -thick lines-, $\vec{\mathbf{D}}, \mathbf{J}_n, \mathbf{J}_p$ -dotted lines-.
- d) carriers concentrations (n and p, log scale) along the structure (dotted lines represents the initial states i.e. concentrations at equilibrium).

Currents for electrons and holes have been computed through different sections along the structure (including extremities, i.e. ohmics contacts) -these currents are very easy to compute in the context of mixed finite elements when the section is composed of triangle edges-. As expected constant values are found (see table 1

Forward bias					
BIAS	I_n	Max deviation		I_p	Max deviation
0.2	$-3.55 * 10^{-17}$	0.25 %		$-7.06 * 10^{-20}$	0.31 %
0.4	$-6.96 * 10^{-14}$	$2. * 10^{-3}$ %		$-1.53 * 10^{-16}$	$2. * 10^{-3}$ %
0.6	$-1.27 * 10^{-10}$	$4. * 10^{-6}$ %		$-1.99 * 10^{-13}$	$5. * 10^{-6}$ %
0.8	$-1.19 * 10^{-7}$	$7. * 10^{-6}$ %		$-7.50 * 10^{-11}$	$7. * 10^{-9}$ %
1.0	$-3.64 * 10^{-5}$	$2. * 10^{-10}$ %		$-1.72 * 10^{-8}$	$5. * 10^{-11}$ %
1.2	$-4.87 * 10^{-3}$	$7. * 10^{-11}$ %		$-3.57 * 10^{-6}$	$5. * 10^{-11}$ %
1.4	$-4.36 * 10^{-1}$	$1. * 10^{-11}$ %		$-5.16 * 10^{-4}$	$8. * 10^{-11}$ %
1.6	$-1.54 * 10^{+1}$	$1. * 10^{-7}$ %		$-5.81 * 10^{-2}$	$5. * 10^{-8}$ %

Table 1: Electron and Hole currents.

where I_n or (I_p) is the mean value of the current through the differents sections, we give also the maximun deviation (percentage) of the computed currents with respect to this mean value). It appears that with the mixed finite element approximation described in this paper, currents can be computed without loss of precision, by direct integration along ohmic contacts.

- **Reverse bias**

  We proceed in this case by continuation on applied voltages (increments 0.2V), starting from the equilibrium state. Figure 7 gives the result obtained for the electrostatic potential, Fermi levels and carriers concentration, for the step $(-0.2V \longrightarrow -0.4V)$ and for $(-1.4V \longrightarrow -1.6V)$. Results concerning currents are reported on table 2. As expected the variation of the currents with respect to the applied bias is extremely much slower than in forward bias. In the case of reverse bias, convergence of ADI algorithm is much slower than for forward bias and it seems -presently- that the determination of distributed time steps is more crucial; as the currents flowing along the structure are extremely low, compatibility problems (problems due to limited machine precision of real numbers) between primal and dual variables for the continuity equations are always present.

Acknowledgements

Authors thank R. Glowinski and P. LeTallec for many fruitful discussions.

Reverse bias				
BIAS	I_n	Max deviation	I_p	Max deviation
0.1	$1.87 * 10^{-20}$	0.23 %	$3.05 * 10^{-23}$	0.22 %
0.2	$2.04 * 10^{-20}$	0.24 %	$3.12 * 10^{-23}$	0.25 %
0.4	$2.43 * 10^{-20}$	0.26 %	$3.13 * 10^{-23}$	0.32 %
0.6	$2.94 * 10^{-20}$	0.27 %	$3.13 * 10^{-23}$	0.33 %
0.8	$3.61 * 10^{-20}$	0.28 %	$3.14 * 10^{-23}$	0.27 %
1.0	$4.53 * 10^{-20}$	0.29 %	$3.14 * 10^{-23}$	0.34 %
1.2	$5.80 * 10^{-20}$	0.27 %	$3.15 * 10^{-23}$	0.33 %
1.4	$7.54 * 10^{-20}$	0.29 %	$3.16 * 10^{-23}$	0.29 %

Table 2: Electron and Hole currents.

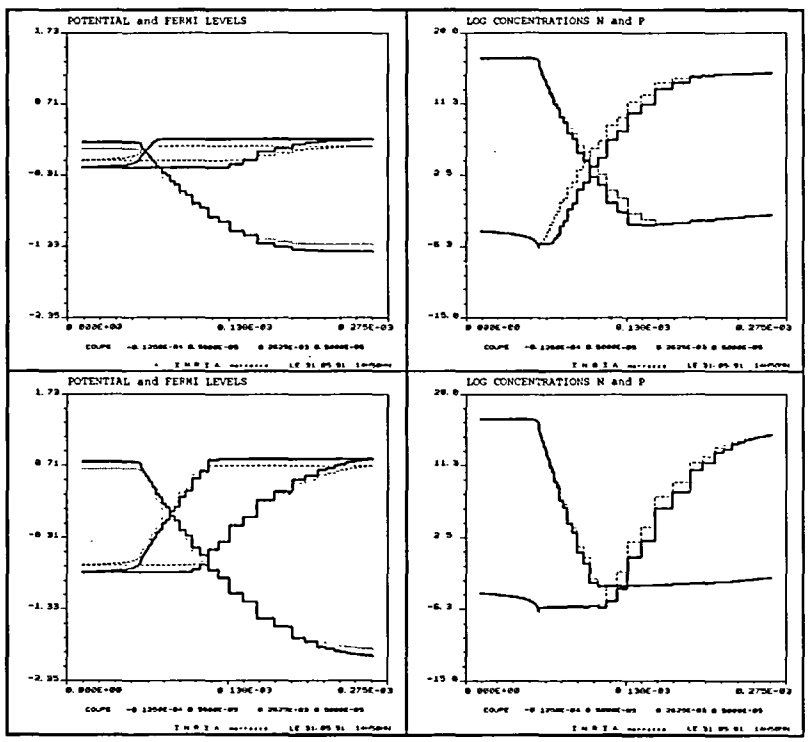

Figure 7: Reverse bias (GaAs diode) 0.4V & 1.6V

References

[1] S. SELBERHERR, *Analysis and Simulation of Semiconductor Devices*, Springer Verlag, Wien (1984).

[2] J.E. VIALLET, *Simulation temporelle de dispositifs à semiconducteurs à hétérojonctions: mise en équation et méthodes numériques*, Thèse de Doctorat ès Sciences Physiques, Paris 6, (1986).

[3] M. FILOCHE, E. CAQUOT, J.F. PALMIER, *ETHER: logiciel de simulation unidimensionnelle du comportement électrique des dispositifs semiconducteurs à hétérojonctions*, Publication CNET, (1988).

[4] P.A. RAVIART, J.M. THOMAS, *A mixed finite element method for 2nd order elliptic problems*, in Mathematical Aspects of Finite Element Methods (I.Galligani and E.Magenes Ed.), Lecture Notes 606, Springer Verlag (1977), pp 292-315

[5] M. FORTIN, R. GLOWINSKI, *Méthodes de lagrangien augmenté. Applications à la résolution de problèmes aux limites*, Dunod, collection Méthodes Mathématiques de l'Informatique n° 9, 1982.

[6] R. GLOWINSKI, P. LE TALLEC, *Augmented Lagrangian and Operator Splitting Methods in Nonlinear Mechanics*, SIAM, Studies in Applied Mathematics, Philadelphia (1989)

[7] R. GLOWINSKI, P. LE TALLEC, *Augmented lagrangian methods for the solution of variational problems*, University of Wisconsin-Madison, MRC Technical report 2965, january 1987.

[8] A.MARROCCO, *Expériences numériques sur des problèmes non linéaires résolus par éléments finis et Lagrangiens Augmentés*, Rapport de recherche IRIA N° 309, mai 1978.

[9] A.MARROCCO, *Semiconductor device modelling using mixed finite elements*, International Workshop, Moscow sept. 90.

This article has been cited by:

1. C. Jourdana, P. Pietra. 2014. A Hybrid Classical-Quantum Transport Model for the Simulation of Carbon Nanotube Transistors. *SIAM Journal on Scientific Computing* **36**:3, B486-B507. [Crossref]
2. F. Brezzi, L.D. Marini, S. Micheletti, P. Pietra, R. Sacco, S. Wang. Discretization of Semiconductor Device Problems (I) 317-441. [Crossref]
3. CLAIRE CHAINAIS-HILLAIRET, YUE-JUN PENG. 2004. FINITE VOLUME APPROXIMATION FOR DEGENERATE DRIFT-DIFFUSION SYSTEM IN SEVERAL SPACE DIMENSIONS. *Mathematical Models and Methods in Applied Sciences* **14**:03, 461-481. [Crossref]
4. J J H Miller, W H A Schilders, S Wang. 1999. Application of finite element methods to the simulation of semiconductor devices. *Reports on Progress in Physics* **62**:3, 277-353. [Crossref]